

Effect of oxide structure on the corrosion behavior of HANA-6 alloys

Jeong-Yong Park¹, Byung-Kwon Choi¹, Seung-Jo Yoo¹, Kyu-Tae Kim² and Yong Hwan Jeong¹
¹*Advanced Core Materials Lab., Korea Atomic Energy Research Institute, Daejeon 305-353, Korea*
²*Korea Nuclear Fuel Co., Ltd., 493 Deokjin-dong, Yuseong-gu, Daejeon 305-353, Korea*
parkjy@kaeri.re.kr

1. Introduction

The burn-up extension of the nuclear fuel is desirable in the context with the economy of reactor operation, but it is hard to be realized without an improvement in the corrosion resistance of the Zr fuel claddings. Such a concern has promoted a great number of researches on the Zr fuel cladding which has produced the development of advanced Zr alloys as a substitute for the Zircalloys [1-4]. In the previous result by the authors [4], the advanced Zr alloy, Zr-1.1wt.%Nb-0.05wt.%Cu which was named HANA-6 showed a much better corrosion resistance when compared to the Zircaloy-4 in various corrosion conditions. However, the corrosion mechanism of the Zr alloys has not really been established so far though a number of empirical relations between the corrosion behavior and the microstructures of the alloy and oxide have been reported by many researchers. The purpose of this study is to enhance the understanding of the corrosion mechanism of Nb-containing Zr alloys.

2. Experimental procedure

Nb-containing Zr alloy with a nominal composition of Zr-1.1wt.%Nb-0.05wt.%Cu (hereafter referred to as HANA-6) was used together with Zircaloy-4 in this study. HANA-6 was fabricated to a cladding tube with an outer diameter of 9.5mm and a wall thickness of 0.57mm while the as-received Zircaloy-4 tube was used. The final annealing for the manufactured HANA-6 tube was applied at three different temperatures, i.e. 470°C, 510°C and 570°C to assess the effect of the final annealing temperature on the corrosion behavior.

Corrosion test of the alloys were performed in a 360°C water condition by using a static autoclave for 1020 days and in a 360°C PWR-simulating loop condition except for the neutron flux for 1000 days. The samples for the corrosion test were cut from the tube into segments with a length of 40mm for HANA-6 and 30mm for Zircaloy-4 and then pickled in a solution of 10 vol.% HF, 30 vol.% H₂SO₄, 30 vol.% HNO₃ and 30 vol.% H₂O.

After the corrosion tests, the cross-section of the oxide was observed by a variety of methods such as a conventional optical microscopy (OM), transmitted light optical microscopy (TLOM) and transmission electron microscopy (TEM).

3. Results and discussion

The corrosion behavior of the HANA-6 and Zircaloy-4 was investigated in 360°C water for 1020 days and in the PWR-simulating loop condition for 1000 days. HANA-6 showed a much lower corrosion rate than Zircaloy-4 irrespective of the final annealing temperature although the corrosion rate of HANA-6 increased with an increase of the final annealing temperature. The weight gain of the 470°C-annealed HANA-6 which showed the lowest corrosion rate was less than 1/3 of that of the Zircaloy-4 corroded for the same duration.

HANA-6 showed a much lower corrosion rate than Zircaloy-4 also in the PWR-simulating loop conditions. The corrosion rate of HANA-6 was increased with an increase of the final annealing temperature in both conditions, but the increment of the corrosion rate with the final annealing temperature was relatively small in the PWR-simulating loop when compared to the 360°C static water. All the alloys showed a lower corrosion rate in the PWR-simulating loop condition than the 360°C static water. This was caused by the fact that the dissolved oxygen concentration in the PWR-simulating loop was maintained below 5 ppb which is much lower than 8 ppm in the static autoclave. Therefore, it is suggested that the corrosion rate of the Zr alloys is highly dependant on the dissolved oxygen content even though the temperature is identical.

Fig. 1 shows the optical micrographs of the oxide cross-section of the HANA-6 and Zircaloy-4. The reflected light optical micrographs showed that the interface of the HANA-6 was smoother than that of the Zircaloy-4. Meanwhile, the transmitted light optical micrographs revealed that the oxide consisted of many layers, which was not seen from the reflected light optical micrographs. The layer structure in the transmitted light optical microscopy would have resulted from the fact that the transparency of the oxide is changed periodically, which is closely related the changes of the grain morphology [5]. The transmitted light would have scattered more in the smaller-sized equiaxed grains when compared to the columnar grains. It implies that the grain morphology is changed periodically when the oxide grows [6].

In the oxide of the HANA-6, there existed two layers with different thicknesses. It was thought that the thicker

layer was fully-developed whereas the thinner one adjacent to the interface is still developing. However, the oxide of the Zirclaoy-4 was found to have six layers with an almost identical thickness. The most important factor that can be related to the corrosion behavior is thought to be the thickness of the fully-developed layer which was higher in the oxide of the HANA-6, indicating that the oxide can become even thicker before an oxide transition in the HANA-6 when compared to the Zircaloy-4.

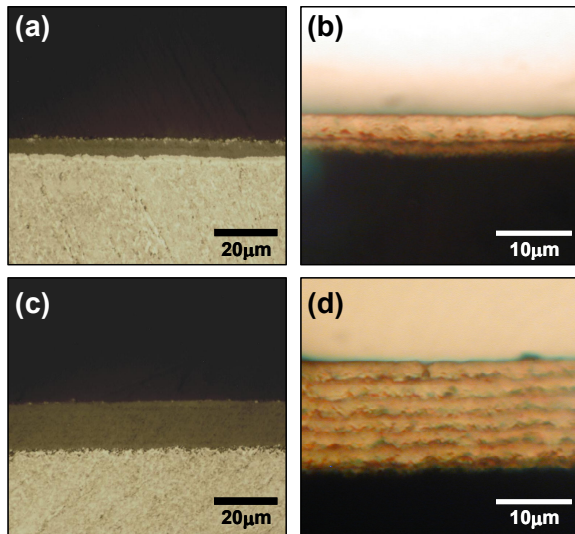


Figure 1. (a,c) Reflected and (b,d) transmitted light optical micrographs on the cross-section of the oxide formed on the (a,b) HANA-6 annealed at 470°C for 8 h and (c,d) Zircaloy-4 after a corrosion test for 1000 days in the PWR-simulating loop conditions.

The oxide transition is usually accompanied by a cracking in the oxide [5] since the stress accumulated during the oxide growth has to be relaxed. Therefore, the oxide of the HANA-6 would withstand a higher stress before a transition or the stress accumulation in the oxide would be lower in the HANA-6 when compared to Zircaloy-4. Although an exact explanation is unavailable at the present stage, it is suggested that the resistance to a cracking is higher in the oxide of HANA-6.

It was well known that Zr alloys exhibit a different corrosion resistance depending on the precipitate characteristics. The precipitates are oxidized after they are incorporated into the oxide because the precipitates are usually more resistant to a oxidation when compared to the Zr matrix. The grain morphology as well as the oxide crystal structure of the oxide is significantly influenced by a delayed oxidation of the precipitate in the oxide. However, the influence of the precipitate on the oxide is different depending on the precipitate characteristics.

We observed $Zr(Fe,Cr)_2$ precipitates located at about 500nm away from the interface in the Zircaloy-4 corroded

in the PWR-simulating loop for 1000 days. The $Zr(Fe,Cr)_2$ precipitate was found to be oxidized from the EDS results. It was also found that there existed many cracks in the vicinity of the oxidized $Zr(Fe,Cr)_2$. On the other hand, the β -Nb located at a similar distance from the interface in the oxide of the HANA-6 maintained a metallic state with no cracks nearby. It implies that $Zr(Fe,Cr)_2$ is more easily oxidized in the oxide of Zircaloy-4 when compared to the β -Nb in HANA-6.

4. Conclusions

The corrosion behavior and the oxide properties of HANA-6 (Zr-1.1wt.%Nb-0.05wt.%Cu) and Zircaloy-4 have been investigated. The corrosion rate of the HANA-6 alloy was much lower than that of the Zirclaoy-4 in a 360°C water and a 360°C PWR-simulating loop condition. It was observed that the oxides of the HANA-6 and the Zircaloy-4 consisted of two and six layers, respectively, after 1000 days in the PWR-simulating loop and the thickness of a fully-developed layer was higher in the HANA-6 than in the Zircaloy-4. β -Nb in HANA-6 was oxidized more slowly when compared to $Zr(Fe,Cr)_2$ in Zirclaoy-4 when the precipitates incorporated into the oxide were observed by TEM.

Acknowledgements

This study was supported by KOSEF and MOST, Korean government, through its National Nuclear Technology Program.

REFERENCES

- [1] G.P. Sabol, G.R. Kilp, M.G. Balfour, E. Roberts, ASTM STP 1023 (1989) 227.
- [2] J.-P. Mardon, D. Charquet, J. Senevat, ASTM STP 1354 (2000) 505.
- [3] K. Yamate, A. Oe, M. Hayashi, T. Okamoto, H. Anada, S. Hagi, Proc. of the 1997 International Topical Meeting on LWR Fuel Performance (1997) 318.
- [4] J.Y. Park, B.K. Choi, Y.H. Jeong, K.T. Kim, Y.H. Jung, Proc. of 2005 Water Reactor Fuel Performance Meeting (2005) 188.
- [5] A.T. Motta, A. Yilmazbayhan, R.J. Comstock, J.M. Partezana, G.P. Sabol, B. Lai, Z. Cai, J. ASTM Int. 2 (2005) Paper ID JAI12375.
- [6] A. Yilmazbayhan, E. Breval, A.T. Motta, R.J. Comstock, J. Nucl. Mater. 349 (2006) 265.